INVESTIGATION OF BAIKDU-SAN VOLCANO WITH SPACE-BORNE SAR SYSTEM

Duk-Jin Kim, Lanying Feng and Wooil M. Moon
Dept. of Earth System Science, Seoul National University, Seoul 151-742, Korea
(djkim@eos1.snu.ac.kr; wmoon@eos1.snu.ac.kr)

Abstract

Baikdu-san was a very active volcano during the Cenozoic era and is believed to be formed in late Cenozoic era. Recently it was also reported that there was a major eruption in or around 1002 A.D. and there are evidences which indicate that it is still an active volcano and a potential volcanic hazard.

Remote sensing techniques have been widely used to monitor various natural hazards, including volcanic hazards. However, during an active volcanic eruption, volcanic ash can basically cover the sky and often blocks the solar radiation preventing any use of optical sensors. Synthetic aperture radar(SAR) is an ideal tool to monitor the volcanic activities and lava flows, because the wavelength of the microwave signal is considerably longer that the average volcanic ash particle size.

In this study we have utilized several sets of SAR data to evaluate the utility of the space-borne SAR system. The data sets include JERS-1(L-band) SAR, and RADARSAT(C-band) data which included both standard mode and the ScanSAR mode data sets. We also utilized several sets of auxiliary data such as local geological maps and JERS-1 OPS data. The routine preprocessing and image processing steps were applied to these data sets before any attempts of classifying and mapping surface geological features. Although we computed sigma nought (σ^0) values for the standard mode RADARSAT data, the utility of sigma nought image was minimal in this study. Application of various types of classification algorithms to identify and map several stages of volcanic flows was not very successful. Although this research is still in progress, the following preliminary conclusions could be made: (1) sigma nought (RADARSAT standard mode data) and DN (JERS-1 SAR and RADARSAT ScanSAR data) have limited usefulness for distinguishing early basalt lava flows from late trachyte flows or later trachyte flows from the old basement granitic rocks around Baikdu-san volcano, (2) surface geological structure features such as several faults and volcanic lava flow channels can easily be identified and mapped, and (3) routine application of unsupervised classification methods cannot be used for mapping any types of surface lava flow patterns.

Keywords: Baikdu-san (or Changbai-san), volcano, SAR, RADARSAT, JERS-1 SAR, volcanic hazard

1. INTRODUCTION

Space-borne SAR (synthetic Aperture Radar) has recently become very effective research tool in many Earth science disciplines, particularly in geological applications such as lithological mapping and structural geological mapping, non-renewable resource exploration, geomorphology, Glacial geology, and geological hazard monitoring and predication. One of the main advantages of space-borne SAR systems is the all weather 24 hour continuous Earth observation capability. Recently a number of such new Earth observation satellites with SAR systems, have become available, which include ERS-1, JERS-1, ERS-2, RADASAT and limited availability of NASAs Shuttle payloads (SIR-C). Also, new advances in sensor development and in data processing and imaging techniques are expected to open more new application developments in geological hazard monitoring and disaster management research.

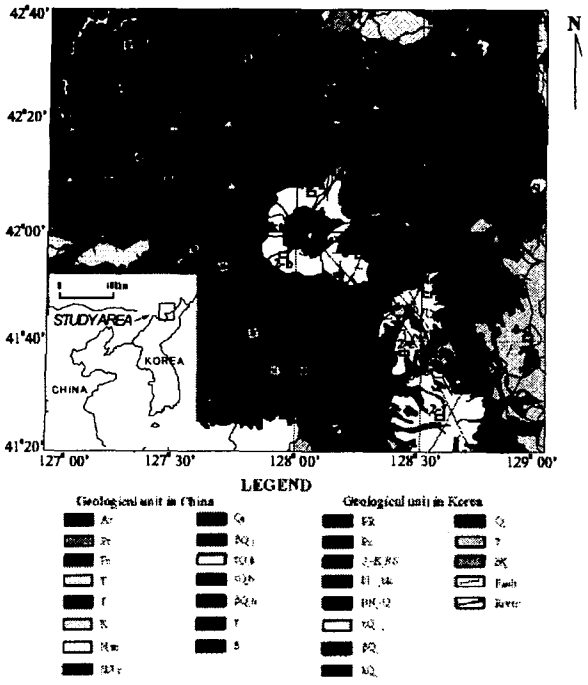

Fig. 1. Geology Map of the Baikdu-san area.

In this study, we have investigated application of traditional remote sensing techniques and space-borne SAR data for characterization of surface geological

material of Baikdu-san volcano in Northeastern China (This volcano is also called Changbai-san in China). Baikdu-san (Changbai-san) at the geographical boundary of China and North Korea was a very active volcano during the Cenozoic era and is believed to be formed sometime in late Cenozoic era. Recently it was also reported that there was a major eruption in or around 1002 A.D. Recent discoveries of volcanic ash formations in the islands of Japan, which are located at least 700km-2,000 km away from the eruption center have proved its origin to be from the 1002 AD eruption of the Baikdu-san. This type of new discoveries provide us with an excellent opportunity to study environmental impact of a major volcanic eruption in view of the newly available satellite data and intelligent GIS tools. The main objective of this paper is to report usefulness of the space-borne (JERS-1 L-band and RADARSAT C-band) SAR systems as remote sensing tools for studying volcano and furthermore studying feasibility of an integrated geological and microwave remote sensing approach of investigating the Baikdu-san volcanism.

2. GEOLOGY OF THE STUDY AREA

1) Geographical Location of the Study Area

Geographic coordinate of the study area, including the Baikdu-san volcano is 127° 00-129° 00 E longitude and 41° 20-42° 40 N latitude. It can be divided into three geomorphic units: central Baikdu-san volcanic cone, piedmont dipped lava plateau, and lava platform. These units are distributed in an approximately concentric form around the volcanic crater lake (Cheonji) (Jin et al., 1994). The altitude of the central volcanic cone is over 2,700 m above mean sea level, the radius of the cone at the base is approximately 20 km, and Choenji, the crater lake, at the top of the cone has an altitude of 2,187 m on average. There are 16 peaks around the crater lake (Fig. 1).

2) Geology

Baikdu-san is located at the junction of northeastern edge of Huabai tectonic block, eastern Europe-Asia continent and mid-Cenozoic northwestward off-shore Pacific volcanic zone, and have gone through a very slow crustal evolution resulting in a very complicated geological structure. The stratigraphic sequence in the study area includes representation from all ages from Archaean to the Tertiary, as shown in the schematic geology map (Fig. 1). Major geological units, including stratigraphy and igneous intrusions and structural sequences, are shown in Table 1 (Jin et al., 1994).

3. DIGITAL DATA SETS

1) JERS-1 SAR DATA

JERS-1 was launched in 1992 with two sensors: OPS (VNIR, and SWIR) and L-band (1.275 GHz, 23.53 cm) SAR system. One of the main objectives of the JERS-1 design team included the Earth resources mapping. with natural hazard monitoring as a minor objective. The JERS-1's L-band SAR had longer wavelength signal compared to the C-band radar system and it was generally known to be more suitable for geological mapping, specially over heavily vegetated terrain, because of its volume scattering and penetration capability through vegetation canopy. The SAR image data used in this study were two scenes acquired on November 7, 1992, and the other two scene acquired at November 8, 1992. The JERS-1 also had VNIR and SWIR OPS imaging systems. The JERS-1 SAR technical characteristics, relevant to this study, are tabulated in Table 2.

GEOLOGICAL AGE		Symbol	GEOLOGICAL FORMATION
Cenozoic Era	Quaternary	$\beta Q_3 n$ (λQ_3)	Distributed along Tumen River (east of Baiktu-san). Mainly gray black olivine basalt, olivine pyroxene basalt, fumarole olivine basalt
		βQ_3	Olive basalt, pyroxene basalt
		$\tau Q_3 b$	Distributed in Baiktu-san around Choenji, located in the upper strata of volcanic cone. Mainly blue-gray alkali-feldspar trachyte, purple red trachyte, acmite-augite quartz trachyte, and olivine pyroxene basalt
		$\tau Q_3 b$ (τQ_{1-2})	Distributed around Choenji volcanic cone outer. Mainly gray quartz trachyte, tuff, acmite-augite quartz trachyte and residuum clay
		$\beta Q_3 j$	Distributed around Baiktu-san Choenji. Mainly gray basaltic breccia lava, gray black trachyte basalt
		$Q_4(Q_4)$	Quartiary sediment: sand, gravel and surface material
	Tertiary	βN_2-Q_1 $\beta N_2 c$	Distributed in the east of Baiktu-san volcanic cone. Mainly alkali olivine basalt, basanite and olivine tholeiite
		$N_1 m$ $N_1 sbk$	Sand gravel bed, sand and silt clay
Mesozoic Era	Cretaceous	K	Not develop very much, mainly sandstone, sand claystone, andesite and its detrital, contained abundant fossil
	Jurassic	J	Distributed extensively, mainly volcanic rocks, detrital rocks and coal system
	Triassic	T	Intermediate acid volcanic rocks, evolute from intermediate basic to intermediate acid igneous rocks
Palaeozoic Era		Pz	Distributed mostly in south of Baiktu-san. Includs Cambrian series, early Ordovician series, middle late Carboniferous series and Permian series.Rock types include inheritance epicontinental detrital-carbonite, marine and land interfacies-land facies detrital sediment, which produce various animal and plant fossils
Proterozoic Era		Z Pt (PR)	Emerged in small area. Mainly granulite, supergene granulite, plagioclase gneiss, sandstone, siltstone, shalestone and clay-limestone
Archaean Era		Ar	Distributed in the northeast and northwest edge of the study area. Mainly granitic rocks, deep crustal rocks and granite-greenstone zones

Table 1. Geological formation and symbols of the study area

2) RADARSAT

Radarsat SAR system uses C-band (5.3 GHz, 5.7 cm) wavelength and HH Polarization, and has several beam modes and beam types which users can choose. The RADARSAT data used in this study were descending orbit Standard (S5) and ScanSar (SWB) mode data, acquired on March 1, 1998, and February 22, 1998, respectively (Table 2).

3) Geological Map

The geology maps for both northeastern China (Bureau of Geology and Mineral Resources of Gilin Province, China) and North Korea (Geology of Korea, published by the Academy of Science of North Korea) were digitized using AutoCAD utilities for later processing with GIS and image fusion steps. The two geology maps were published by two different agencies in two different countries and most of the geological boundaries and geological formation classifications did not agree. These disagreements were resolved by carefully reading the accompanying reports and by reclassifying the rock types and redrawing the geological boundaries (Fig. 1).

4. DATA PROCESSING

There were a few space-borne image data available for the study area, In this study, JERS-1 L-band SAR data and RADARSAT C-band were chosen because of relatively heavy vegetation cover in most of the study area and also because of the weather situation, which is often covered with rapidly moving cloud cover at high altitudes. One of the serious concerns we had with the SAR data was the speckle problem, particularly with JERS-1 SAR data. To reduce the speckles from the image while preserving the contrast of the original image, we have tried several spatial filters including lowpass frequency filter and speckle filters (Lee, 1981; Touzi et al., 1993; and Moon et al., 1994), including the modified Lee filter. We have also experimented with Frost filter, Enhanced Frost filter, and Enhanced Lee filter (Shi et al., 1994). Experiments with different filter sizes were also carried out and the optimum result was obtained with 7x7 with these data sets. Geometric correction was also carried out employing a least squares method with carefully chosen

	RADARSAT		JERS-1	
	Standard	ScanSar	SAR	OPS(VNIR)
Frequency	C-band 5.3GHz (Wavelength : 5.7cm)		L-band 1.275GHz (Wavelength : 23.53cm)	520-600nm Band 1 630-690nm Band 2 760-860nm Band 3
Polarization	HH		HH	NA
Swath width	100km	440km	75km	
Orbit Period	101 minutes		Approx. 96 minutes	
Repeat Orbit Period	24 days		44 days	
Satellite altitude	798 Km		568 Km	
Incidence angle at scene center	36° - 42°	20° - 46°	Approx. 35°	
Date of Data acquisition	3/01/1998 (UTC)	2/22/1998 (UTC)	11/07/1992 (2) 11/08/1992 (2) (UTC)	
Product Type	S5 (descending) SGF	SWB (descending) SCW		

Table 2. SAR data acquisition parameters.

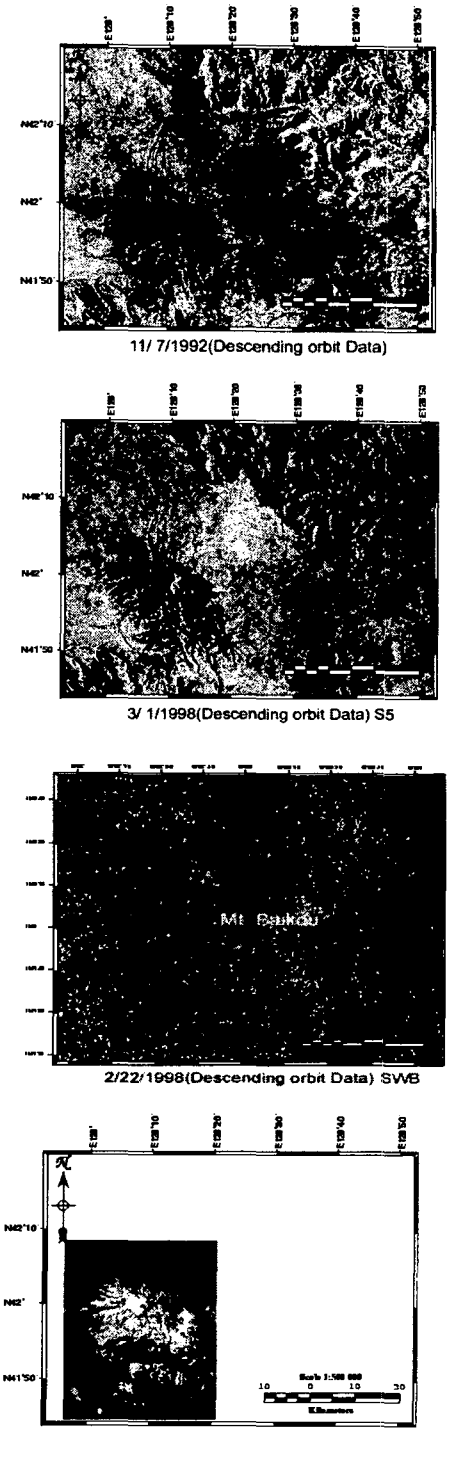

Fig. 2. Data sets over study area. (a) JERS-1 SAR data, (b) RADARSAT Standard data, (c) RADARSAT ScanSAR data, (d) JERS-1 OPS (VNIR) image over the Baikdu-san volcano.

reference points in the study area (Richards, 1993). Geometrically corrected SAR image (Fig. 2(a)(b)(c)(d)) was then overlaid on the digitized geology map for the verification of the processing results and subsequently for the image interpretation (Fig. 3).

5. DISCUSSION

1) Visual Interpretation

The RADARSAT ScanSAR data and a mosaic of four JERS-1 SAR images cover wider areas of the study area and were used for linements and structural feature interpretation. Mapping and verification of the geological structural features were also carried out with the available geological maps as references. As shown in Fig. 4, a number of faults and lava flow channels are clearly shown and imaged. Most of the areas covered by lava is clearly seen although they are mostly covered by reasonably heavy vegetation and farm crops. The lava covered areas usually have bright tone and smooth texture compared the areas of older basement rocks. Although the lava flow channels are clearly outlined, most lava plains have geologically homogeneous appearance. According the to the GIS based calculation, The several stages of lava flows from the Baikdu-san eruption cover an approximate area of 600,000 Ha. The RADARSAT ScanSAR image has low resolution but it covers a much wider area while showing most major geological structural features. However, for detailed investigation, ScanSAR mode was not suitable and JERS-1 and RADARSAT SAR data with resolutions in the range of 18 - 30 m were used.

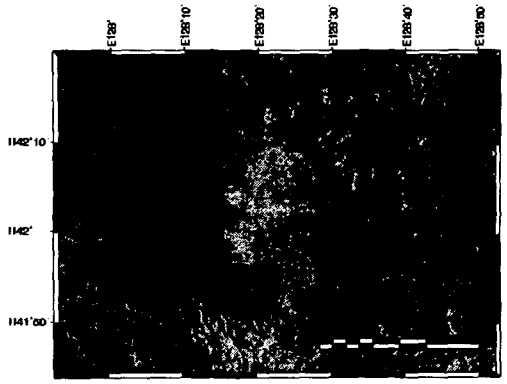

Fig. 3. Composite Geological Map overlaid on RADARSAT image

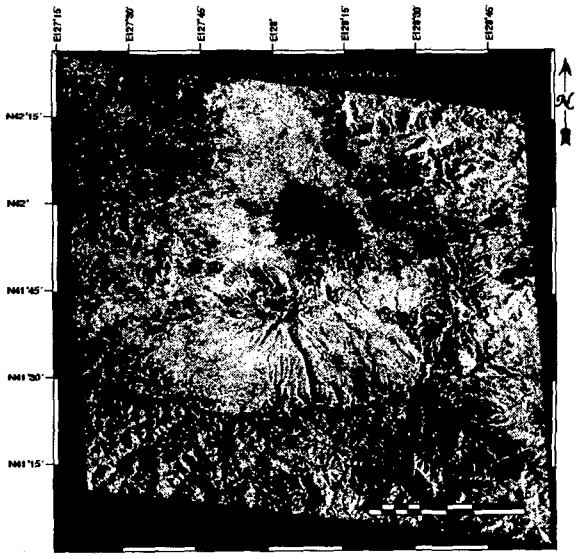

Fig. 4. Lava flow boundary of the JERS-1 SAR mosaic image

2) Microwave backscattering from geological formations

The radar cross section σ, which has units of area, characterizes the scattering strength of the target in the backscattering direction in the form of an effective area. In general, σ of a given target is related to its shape and dielectric constant, the viewing geometry, and the wavelength λ and polarization directions of the incident and scattered waves. The standard definition for σ is in terms of the ratio of the scattered power density $I_{rec}(=\frac{P_t G^t \sigma}{(4\pi R^2)^2})$ measured at a distance R from the scatterer to the power density $I(R)(=\frac{P_t G^t}{4\pi R^2})$ of an incident wave. The P_t is average transmitter power, and the G^t is antenna gain. Thus,

$$\sigma = \lim_{R\to\infty}(4\pi R \frac{I_{rec}}{I(R)})$$

where the limit as $R\to\infty$ is included to denote that the observation point is in the far-field region. In the case of RADARSAT data, the relationship between Digital Number (DN) and radar cross section(σ) is as follow:

$$DN = INT[A_2 . \sqrt{\sigma} + A_3]$$

where A_2(function of range) is the output scaling gain, A_3 is the output scaling offset, which is normally zero. The backscattering coefficient (or sigma nought) is defined as the backscattering cross section of a distributed target of horizontal area A, normalized with respect to A such that $\sigma^0 = \sigma / A$ (Curlander et al., 1991, Ulaby et al., 1989). The sigma nought is calculated as follows:

$$\sigma_j^0 = \beta_j^0 + 10 * \log_{10}(\sin I_j) \ (dB)$$

where

$$\beta_j^0 = 10 * \log_{10}[(DN_j^2 + A3)/A2_j] \ (dB)$$

where I is incidence angle, and index j represents the order of pixel (Srivastava et al., 1998).

Since the sigma nought image could be calculated from RADARSAT data but could not be estimated from JERS-1 SAR because of lack of necessary information. To investigate relative relationships between different volcanic flows, a table of DN (Digital Numbers) for a selected number training sites are made (Table 3). For the upper eruption stage or younger eruptives ($\tau Q_2 b$) distributed in Baikdu-san around Choenji (Fig. 1.<3-a, 3-b>) and located in the upper strata of volcanic cone, have the lowest average DN about 100. But the other three groups have the very similar DNs (Fig. 5.(a)(b)). According to the preliminary investigation in this study, the sigma nought and DNs have limited usefulness for distinguishing early basaltic lava flows from late stage trachytic eruptive flows and also distinguishing the later trachyte flows from the older granite gneissic basement rocks northeast of the Baikdu-san volcano.

In general the average DN and sigma nought values corresponding to each geological units are such that the L-band JERS-1 SAR data have more distinguishable distribution peaks than those of the C-band RADARAT data. Based on this information, JERS-1 SAR will theoretically have more usefulness for the classification of surface geological formations. However, it was also learned that the well known unsupervised classification algorithms are not suitable for automatic mapping of rocks using SAR data. For more effective and accurate identification and mapping, a multi-sensor type data fusion will be necessary.

3) Classification of fresh and old lava flows

The lave fields around the Baikdu-san usually have homogeneous features in most part. In the northeastern part of Baikdu-san, however, there are distinct areas where the JERS-1 SAR data have darker tones where RADARSAT standard mode data have much brighter tone (Fig. 6(a), 6(b)). Because both images were recorded from the descending orbit geometry and similar look angle, the differences can mean a number of different situations. However, one clear conclusion may be that the surface and near surface materials in this particular area backscatter the microwave in different ways. Geologically, however, this can mean either the area is differently weathered from other parts of lava flows and/or the area represents different age lava flows from the surrounding areas. Although we have carried out a limited field work, we could not understand the exact reason.

			JERS-1	RADARSAT	
	Formation	Site	DN	DN	Sigma-nought
Baikdu-san alkaline trachyte	Upper eruption stage	3-b	85	108	-13.562
		3-a	90	100	-14.648
	Lower eruption stage	2-e	131	124	-11.343
		2-d	141	124	-11.409
		2-c	155	132	-10.279
		2-b	132	142	-8.899
		2-a	144	134	-9.933
Bai-san Basalt		1-e	147	140	-9.162
		1-d	171	127	-10.979
		1-c	111	134	-10.021
		1-b	121	133	-10.066
		1-a	116	130	-10.560
Granite rocks		4-d	140	116	-12.402
		4-c	154	134	-9.943
		4-b	153	122	-11.676
		4-a	151	122	-11.671

Table 3. Average DN and sigma-nought values corresponding to each geological formation.

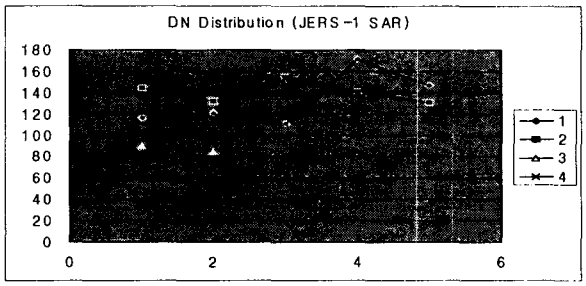

(a)

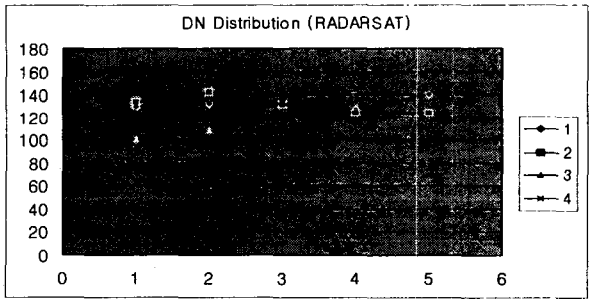

(b)

Fig. 5. (a) DN distribution of JERS-1 SAR, (b) DN distribution of RADARSAT data.

Nevertheless, we have carried out several classification experiments including both unsupervised and supervised classification methods in addition to the principal component analysis (PCA). We have also coded an evidential belief function classification method(Lee et al., 1987) and tested. One of our objectives was to automatically map the different age volcanic flows using the space-borne SAR data. For

this experiment, we utilized all available JERS-1 OPS, JERS-1 SAR, RADARSAT Standard mode and ScanSAR mode data. However, application of various types of classification algorithms to identify and map several stages of volcanic flows was not very satisfactory at this stage.

6. CONCLUSION

This research is still in progress, But some of the preliminary conclusions are made: (1) The total areal extent of the Baikdu-san lava flow is approximately 600,000 Ha, (2) Sigma nought (σ^0) (RADARSAT standard mode data) and DN (JERS-1 SAR and RADARSAT ScanSAR data) have only limited usefulness for distinguishing early basalt lava flows from late trachyte flows or later trachyte flows from the old basement granitic rocks around Baikdu-san volcano, (3) Most surface geological structural features such as faults, volcanic lava flow channels, rift and lava flow boundaries can easily be identified and mapped from all three SAR image data, and (4) Routine application of unsupervised classification methods cannot be used directly for mapping of surface lava flow patterns and may require multi-sensor data fusion.

Reference

J. C. Curlander and R. N. McDonough, 1991, *Synthetic Aperture Radar Systems and Signal Processing*, John Wiley & Sons, Inc.

B. L. Jin and X. Y. Zhang, 1994, *Researching Volcanic Geology in Mount Changbai, Bureau of Geology and Mining*, Jilin Province, China.

J. S. Lee, 1981, *Refined Filtering of Image Noise using Local Statistics, Computer Graphics and Image Processing*, 15, 380-389.

T. Lee, J. A. Richards, and P. H. Swain, 1987, *Probabilistic and Evidential Approaches for Multispectral Data Analysis*, IEEE Trans. Geoscience and Remote Sensing, Vol, GE-25, No.3, pp. 283-293.

W. M. Moon, B. Li, V. Singhroy, C. S. So, and Y. Yamaguchi, 1994, *Notes on JERS-1 SAR Data Characteristics for Geological Applications*, Canadian Jour. Remote Sensing, 20, 329-332.

J. A. Richards, 1993, *Remote sensing Digital Image Analysis*, Springer-Verlag, Berlin.

Z. Shi and K. B. Fung, 1994, *A comparision of Digital Speckle Filters*, Proceedings of IGARSS'94, 2129-2133.

S. Srivastava and N. Shepherd, 1998, *Extraction of Beta Nought and Sigma Nought from RADARSAT CDPF Products*, Rev.2-22 May. Contract No.:9F005-6-0025/001/SN.

R. Touzi and A. Lopes, 1993, *Analysis of Speckle Filtering in Polarimetric SAR Imagery*, Proceedings of IGARSS'93, 1419-1422.

F. T. Ulaby, and M. C. Dobson, 1989, *HandBook of Radar Scattering Statistics for Terrain*, Artech House, INC.

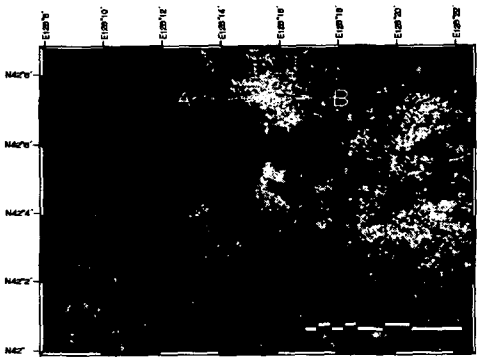

(a)

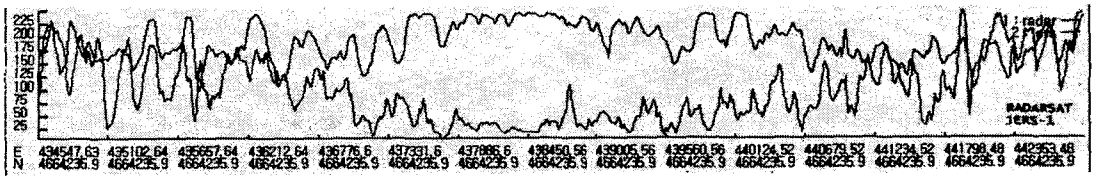

(b)

Fig. 6. (a) DN-difference image between the JERS-1 SAR and RADARSAT image (b) Plot of the DN values along the profile A-B shown in (a)